Nucleosome Remodeling by hMSH2-hMSH6

Sarah Javaid,[1] Mridula Manohar,[2] Nidhi Punja,[1] Alex Mooney,[3] Jennifer J. Ottesen,[2,*] Michael G. Poirier,[1,2,3,*] and Richard Fishel[1,3,*]
[1]Department of Molecular Virology, Immunology, and Medical Genetics, Human Cancer Genetics
[2]Department of Biochemistry
[3]Department of Physics
The Ohio State University and The Ohio State University Medical Center, Columbus, OH 43210, USA
*Correspondence: rfishel@osu.edu (R.F.), mpoirier@mps.ohio-state.edu (M.G.P.), ottesen.1@osu.edu (J.J.O.)
DOI 10.1016/j.molcel.2009.12.010

SUMMARY

DNA nucleotide mismatches and lesions arise on chromosomes that are a complex assortment of protein and DNA (chromatin). The fundamental unit of chromatin is a nucleosome that contains ~146 bp DNA wrapped around an H2A, H2B, H3, and H4 histone octamer. We demonstrate that the mismatch recognition heterodimer hMSH2-hMSH6 disassembles a nucleosome. Disassembly requires a mismatch that provokes the formation of hMSH2-hMSH6 hydrolysis-independent sliding clamps, which translocate along the DNA to the nucleosome. The rate of disassembly is enhanced by actual or mimicked acetylation of histone H3 within the nucleosome entry-exit and dyad axis that occurs during replication and repair in vivo and reduces DNA-octamer affinity in vitro. Our results support a passive mechanism for chromatin remodeling whereby hMSH2-hMSH6 sliding clamps trap localized fluctuations in nucleosome positioning and/or wrapping that ultimately leads to disassembly, and highlight unanticipated strengths of the Molecular Switch Model for mismatch repair (MMR).

INTRODUCTION

Mismatched nucleotides arise in DNA as a result of polymerase misincorporation errors, recombination between heteroallelic parental chromosomes, or chemical and physical damage (Friedberg et al., 2006). MutS homologs (MSHs) and MutL homologs (MLH/PMS) are highly conserved proteins and are essential for the MMR excision reaction that removes mismatches/lesions from DNA (Kolodner et al., 2007). Mutations of hMSH2, hMSH6, hMLH1, and hPMS2 are the causes of a common human cancer predisposition syndrome, hereditary nonpolyposis colorectal cancer (HNPCC; Boland and Fishel, 2005). The hMSH2-hMSH6 heterodimer is required for the initial recognition of mismatches during MMR as well as lesion recognition for specific damage-induced signaling pathway(s) (Drummond et al., 1995; Yoshioka et al., 2006). Although MMR occurs in the context of chromatin in vivo, previous biochemical studies have relied exclusively on naked DNA substrates (Constantin et al., 2005; Zhang et al., 2005). The effect of chromatin on MMR is unknown.

Moreover, no chromatin remodeling activities have been linked to MMR in spite of numerous cellular and genetic surveys (Ataian and Krebs, 2006; Escargueil et al., 2008).

RESULTS

Constructing a Defined Nucleosome-DNA Containing a Mismatch

To determine the effect of nucleosomes on hMSH2-hMSH6 function(s), we have constructed a model DNA substrate containing the *Xenopus* 5S rDNA nucleosome localization sequence linked to a *lacO* sequence, mismatch, and terminal biotin on a 3′ tail (Figure 1A). A single nucleosome was reconstituted on this DNA substrate by salt dialysis, using purified H2A, H2B, H3, and H4 histones that were refolded into histone octamers as previously described (Luger et al., 1999). Nucleosome substrates were formed with three types of histone octamers: those containing no modifications (UN), those containing an acetylation mimic where the H3 lysine-56 is substituted with glutamine (H3[K56Q]), and those containing site-specific acetylation of the histone H3 K115 and K122 residues (H3[K115Ac,K122Ac]). H3(K56) is located in the nucleosome entry-exit region while H3(K115, K122) are located in the nucleosome dyad beneath the wrapped DNA. All three residues appear important for normal replication, transcription, and DNA repair (English et al., 2006; Hyland et al., 2005; Zhang et al., 2003). Site-specific acetylation of histone H3(K115, K122) was accomplished by intein-mediated protein ligation that links a recombinant H3 thioester truncated at L109 with a synthetic peptide containing acetylated K115 and K122; this method generates a native peptide bond and H3 protein sequence (Manohar et al., 2009). The mononucleosome-DNA substrates were then purified on a 5%–30% sucrose gradient (see Figures S1A and S1B available online; Lowary and Widom, 1998). The nucleosome positions were mapped using an ExoIII protection assay and found to largely occupy the 5S rDNA sequence shielding ~145 bp of DNA, as well as a number of lower-frequency positioning sites (Figure S1C). The protection footprint suggests that the nucleosomes are composed of histone octamers, and the additional positioning sites appear consistent with the gel migration pattern (Figure S1B).

hMSH2-hMSH6 Binds to Nucleosome-DNA Containing a Mismatch

To determine the effect of nucleosomes on the initiation of MMR, we examined hMSH2-hMSH6 binding to the nucleosome-DNA
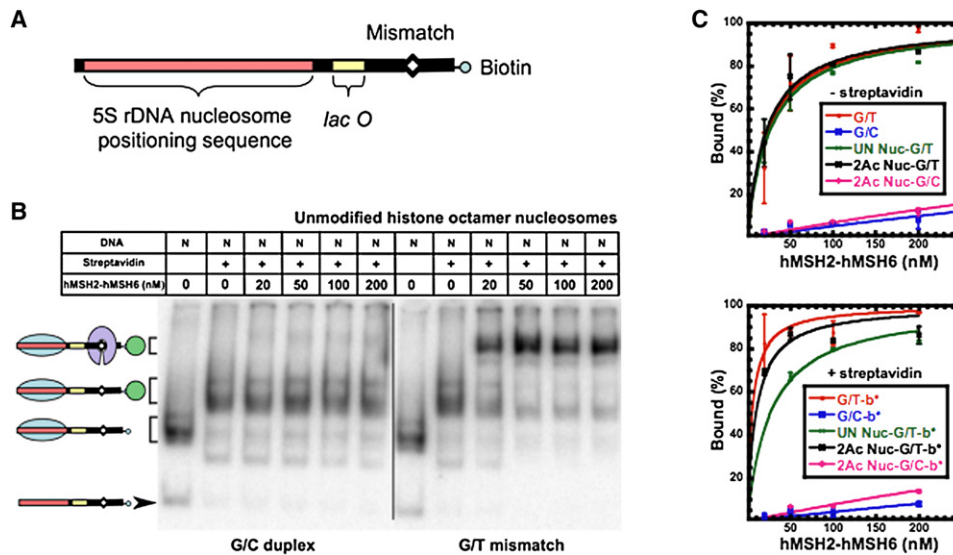
Figure 1. Binding of hMSH2-hMSH6 to Nucleosome-DNA

(A) The nucleosome-DNA substrate contains 17 bp 3′ of the 147 bp 5S rDNA nucleosome localization sequence (red) followed by a 28 bp linker, 24 bp *lacO* sequence (yellow), and 47 bp containing a mismatch site 20 bp from the 3′ end that contains a terminal biotin (light blue).

(B) Representative gel showing specific binding of hMSH2-hMSH6 to the G/T mismatch nucleosome-DNA substrate containing an unmodified nucleosome. Boxes above indicate added reaction components (+), the concentration of hMSH2-hMSH6 (nM), and the inclusion of nucleosome-DNA (N). A schematic of DNA species with arrows or brackets indicating gel mobility position is shown on the left. The DNA substrate is colored as shown in (A) with a nucleosome (blue oval), hMSH2-hMSH6 (purple clamp), and streptavidin (green circle).

(C) Quantitative analysis of hMSH2-hMSH6 binding to free-DNA containing a G/T mismatch (G/T) or G/C duplex (G/C) without or with biotin-streptavidin (-b*) on the 3′ end, and nucleosome-DNA with an unmodified (UN) or H3(K115Ac,K122Ac)-modified (2Ac) nucleosome without or with (-b*). Standard deviations were determined from at least three independent experiments and error bars shown (some within the symbol).

substrates (Figures 1B and 1C). We found little difference in hMSH2-hMSH6 mismatch binding between the free-DNA substrate and the UN and H3(K115Ac,K122Ac) nucleosome-DNA substrates (Figures 1B and 1C; $K_{D\ (G/T)}$ = 24 nM; $K_{D\ (G/T•b•UN)}$ = 27 nM; $K_{D\ (G/T•b•K115Ac/K122Ac)}$ = 22 nM), and in the presence of streptavidin that induces a physical block to one end of the DNA substrate (Figure 1C; $K_{D\ (G/T•b-SA•UN)}$ = 26 nM; $K_{D\ (G/T•b-SA•K115Ac/K122Ac)}$ = 10 nM). The binding of hMSH2-hMSH6 to identical DNA substrates without the mismatch (G/C) was over 50-fold less efficient (Figures 1B and 1C; $K_{D\ (G/C)}$ = 1808 nM; $K_{D\ (G/C•b•K115Ac/K122Ac)}$ = 1342 nM; $K_{D\ (G/C•b-SA•K115Ac/K122Ac)}$ = 1198 nM). Similar mismatch-specific binding was observed for the H3(K56Q) nucleosome-DNA substrate. These results demonstrate that the nucleosome-DNA substrates containing a mismatch outside of the predominant nucleosome localization region are efficiently recognized by hMSH2-hMSH6.

The addition of ATP to hMSH2-hMSH6 bound to a mismatch provokes the formation of a hydrolysis-independent sliding clamp that may diffuse off an open DNA end (Gradia et al., 1999; Mendillo et al., 2005; Selmane et al., 2003). ATP-dependent release of the sliding clamp from the mismatch allows iterative cycles of hMSH2-hMSH6 loading and clamp formation (Acharya et al., 2003; Gradia et al., 1999, 2000). These iterative cycles can result in multiple ATP-bound hMSH2-hMSH6 clamps that may be trapped on the DNA by blocking the ends with biotin-streptavidin or by using a circular DNA substrate (Acharya

et al., 2003; Gradia et al., 1999; Mendillo et al., 2005; Schofield et al., 2001).

Nucleosomes are highly stable protein-DNA complexes that are known to sterically occlude DNA-binding proteins from their target sites (Li and Widom, 2004; Polach and Widom, 1995; Utley et al., 1996). The ability of a nucleosome to block the diffusion of hMSH2-hMSH6 sliding clamps and potentially impede MMR is a significant unknown. Consistent with previous work, we found that addition of streptavidin to a free-DNA (F) substrate containing a single biotin on the 3′ tail resulted in a mobility shift (Figures 2A–2C, compare lanes 1 and 2; Figures S2A and S2B, compare lanes 1 and 2; Gradia et al., 1999). An additional mismatch-specific shift on this single end-blocked DNA was observed with hMSH2-hMSH6 (Figures 2A–2C, lane 3; compared to Figures S2A and S2B, lane 3) that was released from the remaining open end of the DNA substrate with the addition of ATP (Figures 2A–2C, lane 4). These results are consistent with previous studies that demonstrated a single biotin-streptavidin blocked end is not sufficient to retain ATP-bound hMSH2-hMSH6 sliding clamps on mismatched DNA (Gradia et al., 1999). We found that the unmodified, H3(K56Q) modification mimic, or H3(K115Ac,K122Ac)-modified nucleosome-DNA substrate (N) with an open 3′ tail, behaved similarly to the free-DNA (F) substrate containing a single biotin-streptavidin blocked end (Figures 2A–2C, compare lanes 2–4 with lanes 5–7; Figures S2A and S2B, lanes 5–7). In this case, the nucleosome-DNA substrate (Figures 2A–2C, lane 5) was bound specifically with
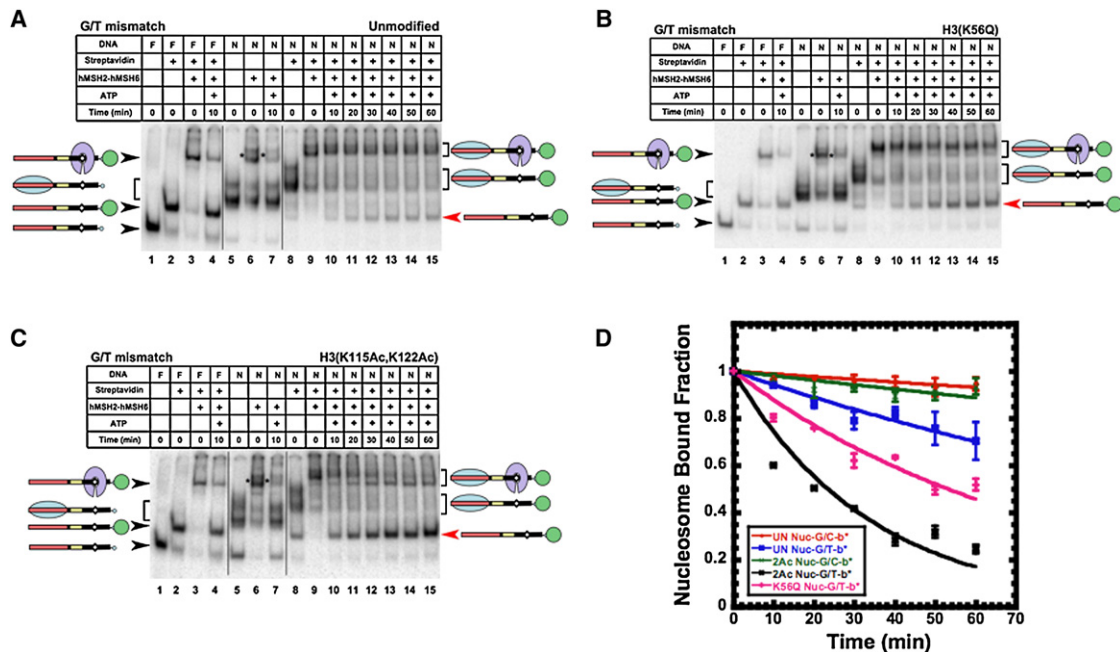
Figure 2. Nucleosome Disassembly by hMSH2-hMSH6

(A–C) Representative gels showing the nucleosome disassembly reaction catalyzed by hMSH2-hMSH6 with (A) G/T mismatch nucleosome-DNA containing an unmodified nucleosome, (B) G/T mismatch nucleosome-DNA containing an H3(K56Q) acetylation mimic nucleosome, and (C) G/T mismatch nucleosome-DNA containing an H3(K115Ac,K122Ac)-modified nucleosome. Black bars indicate image splicing from a single gel where spliced out lanes were redundant with Figure 3B. Boxes above indicate added reaction components (+) and the inclusion of free-DNA (F) or nucleosome-DNA (N). A schematic of DNA species with arrows or brackets indicating gel mobility position is shown on the left and right of the gel panels. The DNA substrate is colored as shown in Figure 1A with a nucleosome (blue oval), hMSH2-hMSH6 (purple clamp), and streptavidin (green circle). Asterisks indicate the mobility of nucleosome-DNA substrate with bound hMSH2-hMSH6 and without a biotin-streptavidin-bound 3′ tail. Red arrow indicates the gel mobility of the nucleosome disassembly product. Asterisk (*) indicates the position of the nucleosome substrate bound by hMSH2-hMSH6; multiple bands are consistent with multiple nucleosome positions surrounding the 5S rDNA localization site (see Figure S1).

(D) Quantitative analysis of the nucleosome disassembly reactions. Data analysis includes representative gels shown in (A) and (B) as well as Figure S2. Each data set was fit to a single exponential decay to calculate τ and $t_{1/2}$. Key: unmodified nucleosome substrate containing duplex DNA (G/C) and biotin-streptavidin blocked (b*) 3′ tail (UN Nuc-G/C-b*), unmodified nucleosome substrate containing a G/T mismatch and biotin-streptavidin-blocked 3′ tail (UN Nuc-G/T-b*), H3(K56Q) acetylation mimic nucleosome substrate containing a G/T mismatch and biotin-streptavidin-blocked 3′ tail (K56Q Nuc-G/T-b*), H3(K115Ac,K122Ac) nucleosome substrate containing duplex DNA (G/C) and biotin-streptavidin-blocked 3′ tail (2Ac Nuc-G/C-b*), and H3(K115Ac,K122Ac) nucleosome substrate containing a G/T mismatch and biotin-streptavidin-blocked 3′ tail (2Ac Nuc-G/T-b*). Standard deviations were determined from at least three independent experiments and error bars shown (some within the symbol).

hMSH2-hMSH6 (see asterisk, Figures 2A–2C, lane 6; compare Figures S2A and S2B, lane 6), which was then released upon addition of ATP (Figures 2A–2C, lane 7).

Nucleosome Disassembly Is Catalyzed by hMSH2-hMSH6

To determine whether nucleosomes blocked the sliding of hMSH2-hMSH6 clamps, we examined the nucleosome-DNA substrates containing biotin-streptavidin blocked 3′ tails (Figures 2A–2C, lanes 8–15; Figures S2A and S2B, lanes 8–15). Nucleosome stability may be calculated from data with the nucleosome-DNAs containing a G/C duplex, where hMSH2-hMSH6 displays insignificant binding activity (Figures S2A and S2B, lanes 8–15; $t_{1/2\ (G/C\bullet UN)}$ = 578 min, $t_{1/2\ (G/C\bullet K115Ac/K122Ac)}$ = 347 min; Figure 2D). These results demonstrate that unmodified and H3(K115Ac,K122Ac)-modified nucleosomes are stable for 10–20 hr under our experimental conditions. A similar stability is observed with H3(K56Q) nucleosomes (data not shown).

In contrast, we found that incubation of the biotin-streptavidin blocked G/T mismatch nucleosome-DNA substrates with hMSH2-hMSH6, and ATP resulted in the eviction of the histone octamer (Figures 2A–2C, lanes 8–15, red arrow; quantified in Figure 2D). These results suggest that a nucleosome does not block ATP-bound hMSH2-hMSH6 sliding clamps and that the nucleosome appeared to be disassembled by hMSH2-hMSH6. Moreover, there was a significant difference in the ability of hMSH2-hMSH6 to disassemble unmodified versus the H3(K56Q) mimic or H3(K115Ac,K122Ac)-modified nucleosomes (Figure 2D; $t_{1/2\ (G/T\bullet UN)}$ = 117 min, $t_{1/2\ (G/T\bullet K56Q)}$ = 53 min, $t_{1/2\ (G/T\bullet K115Ac/K122Ac)}$ = 23 min, respectively). Our previous work has demonstrated that H3(K115Ac,K122Ac) increases the rate of thermal repositioning and reduces the DNA-histone binding free energy compared to unmodified nucleosomes (Manohar et al., 2009). These observations are consistent with the conclusion that nucleosomes containing H3 acetylation mimics and/or modifications that reduce their intrinsic DNA
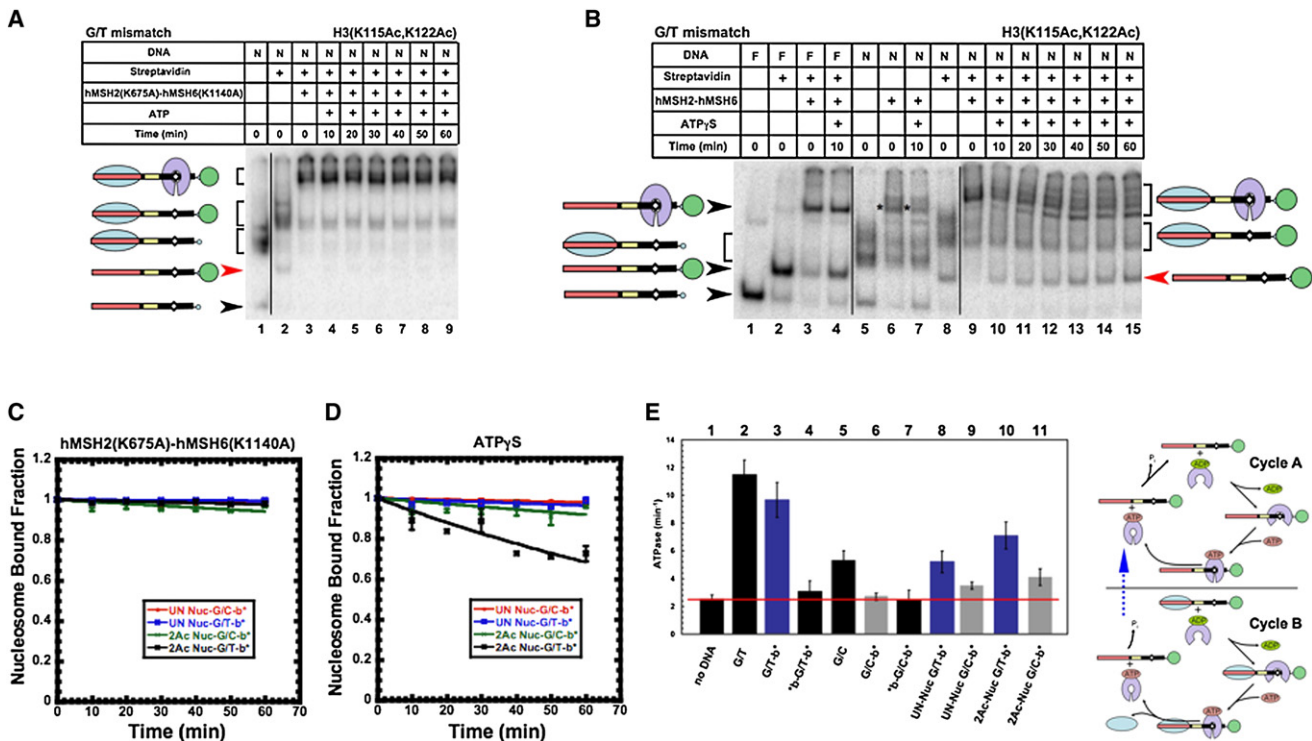
Figure 3. Analysis of the ATP Requirement for hMSH2-hMSH6 Nucleosome Disassembly

Boxes above indicate added reaction components (+), the inclusion of free-DNA (F) or nucleosome-DNA (N), and the time of incubation (min). A schematic of DNA species with arrows or brackets indicating gel mobility position is shown on the left and right of the gel panels. The DNA substrate is colored as shown in Figure 1A with a nucleosome (blue oval), hMSH2-hMSH6 (purple clamp), and streptavidin (green circle). Asterisks indicate the mobility of nucleosome-DNA substrate with bound hMSH2-hMSH6 and without a biotin-streptavidin-bound 3′ tail. Red arrow indicates the gel mobility of the nucleosome disassembly product.

(A) Nucleosome disassembly by hMSH2(K675A)-hMSH5(K1140A). Black bar indicates image splicing from a single gel where spliced lanes contained redundant controls shown in Figures 2A, 2B, and 3B (lanes 6 and 7).

(B) Nucleosome disassembly by hMSH2-hMSH6 in the presence of ATPγS.

(C and D) Quantitative analysis of (A) plus Figures S4A–S4C and (B) plus Figures S4D–S4F, respectively. Each data set was fit to a single exponential decay to calculate τ and $t_{1/2}$. See Figure 2 for key. Standard deviations were determined from at least three independent experiments and error bars shown (some within the symbol).

(E) hMSH2-hMSH6 steady-state ATPase activity. hMSH2-hMSH6 ATPase activity was determined in the absence of DNA (no DNA), with free-DNA containing a G/T mismatch (G/T) or G/C duplex (G/C) with one (-b*) or two (*b-X-b*) biotin-streptavidin blocked ends, or with nucleosome-DNA containing an unmodified (UN-Nuc) or H3(K115Ac, K122Ac)-modified (2Ac-Nuc) nucleosome and a G/T mismatch (G/T) or G/C duplex (G/C) without or with (-b*) a biotin-streptavidin blocked 3′ end. Standard deviations were determined from at least three independent experiments and error bars shown. A diagram of two ATPase cycles is shown on the right. Cycle A illustrates an ATPase cycle for free-DNA containing a single biotin-streptavidin-blocked 3′ end (Gradia et al., 1999). Cycle B illustrates a hypothetical requirement for disassembly of a nucleosome from nucleosome-DNA containing a biotin-streptavidin-blocked 3′ end to complete an ATPase cycle consistent with the data. The dashed blue arrow shows that the two cycles are connected by the product of nucleosome disassembly, which is identical to free-DNA containing a single biotin-streptavidin blocked 3′ end that initiates cycle A.

affinity may be disassembled more efficiently by hMSH2-hMSH6.

ATP Binding by hMSH2-hMSH6 Is Required for Nucleosome Disassembly

ATP-dependent chromatin remodeling is required for numerous cellular DNA transactions including transcription, replication, and repair (Groth et al., 2007). Disassembly of a nucleosome from a localized region on DNA suggests that hMSH2-hMSH6 performs a chromatin remodeling reaction. To explore the mechanism behind this hMSH2-hMSH6 function, we examined the ATP requirement for chromatin remodeling (Figure 3, Figure S3). The hMSH2(K675A)-hMSH6(K1140A) mutant hetero-

dimer binds mismatched DNA similar to the wild-type heterodimer but is incapable of ATP binding and/or hydrolysis (N.P., S.J., and R.F., unpublished data; Haber and Walker, 1991). We found that in spite of a normal mismatch binding activity, hMSH2(K675A)-hMSH6(K1140A) was incapable of catalyzing the disassembly of unmodified or H3(K115Ac,K122Ac)-modified nucleosomes (Figures 3A and 3C, Figures S3A–S3C). These results suggest that ATP binding and/or hydrolysis is required for hMSH2-hMSH6 catalyzed chromatin remodeling. Since the hMSH2(K675A)-hMSH6(K1140A) protein was purified by an identical method to the wild-type protein, these results also imply that preparation contaminants are unlikely to be responsible for the chromatin remodeling activity.

To examine the role of ATP hydrolysis on hMSH2-hMSH6 chromatin remodeling activity, we performed nucleosome disassembly studies with the ATP analog adenosine 5′-[γ-thio]-triphosphate (ATPγS). We determined that the rate of ATPγS hydrolysis (k_{cat}) by hMSH2-hMSH6 in the absence of DNA (0.04 ± 0.02 min^{-1}) or in the presence of mismatched DNA (0.06 ± 0.05 min^{-1}; Figure S4A) and compared it to the well-known rate of ATP hydrolysis in the absence of DNA (1 ± 0.5 min^{-1}) or in the presence of mismatched DNA (22 ± 1.2 min^{-1}; Mazurek et al., 2009). These results clearly demonstrate that hMSH2-hMSH6 is more than 350-fold less capable of hydrolyzing ATPγS compared to ATP when a mismatch is present, and that repeated rounds of mismatch-dependent hydrolysis are dramatically suppressed by ATPγS. Perhaps more importantly, ATPγS is the only analog of ATP that appears to bind hMSH2-hMSH6 and provoke the formation of a sliding clamp similar to ATP, although the kinetics of sliding clamp formation appear slower than ATP (Figure S4B; Gradia et al., 1997).

Control reactions with free DNA demonstrated streptavidin binding (Figure 3B, compare lanes 1 and 2), specific mismatch binding by hMSH2-hMSH6 (Figure 3B, lane 3), and the release of hMSH2-hMSH6 upon addition of ATPγS (Figure 3B, lane 4). These results are similar to previous studies and are consistent with the conclusion that ATP binding by hMSH2-hMSH6 results in the formation of a hydrolysis-independent sliding clamp (Gradia et al., 1999; Mendillo et al., 2005; Selmane et al., 2003). In addition, the single nucleosome substrate DNA containing a G/T mismatch (Figure 3B, lane 5) specifically binds hMSH2-hMSH6 (see asterisk, Figure 3B, lane 6) that is largely released upon the addition of ATPγS (Figure 3B, lane 7). We note that for both the free DNA and the nucleosome-DNA substrates the efficiency of ATPγS-induced release appears reduced compared to ATP. These observations are consistent with kinetic analysis (Figure S4B; Gradia et al., 1997) and suggest that the nucleosome-DNA substrates provoke hMSH2-hMSH6 to form a sliding clamp in the presence of ATPγS, which although modestly slower appears nearly identical to single biotin-streptavidin blocked-end free DNA (Figure 3B, compare lanes 1–4 with lanes 5–7). The addition of ATPγS to the prebound hMSH2-hMSH6 in a chromatin remodeling reaction suggests reduced but significant nucleosome disassembly (Figure 3B, lanes 8–15; $t_{1/2}$ (G/T•K115Ac/K122Ac) = 108 min; Figure 3D; Figures S3D–S3F). Contrasting the ∼4-fold slower rate for nucleosome disassembly in the presence of ATPγS to the ∼350-fold slower rate of ATPγS hydrolysis compared to ATP (Figure S4C), and assuming that the rate-limiting step(s) of the disassembly reaction remains similar, these observations support the notion that γ-phosphate hydrolysis is unlikely to be a significant contributor to the disassembly process. It is important to note that these studies are complicated by a competitive ATPγS *prebinding* reaction that inactivates hMSH2-hMSH6 mismatch binding and freezes iterative mismatch-dependent loading of sliding clamps, which may ultimately contribute to the reduced rate of ATPγS-induced nucleosome disassembly (Acharya et al., 2003; Gradia et al., 1999). Taken as a whole, these observations are consistent with the conclusion that ATP binding, and not hydrolysis, is the most significant contributor to hMSH2-hMSH6 chromatin

remodeling, and that iterative ATP binding likely sustains an efficient reaction.

In the absence of DNA, hMSH2-hMSH6 displays an intrinsic low-level ATP hydrolysis (ATPase) activity (Figure 3E, bar 1) that is stimulated by mismatched DNA (Figure 3E, lane 2). This mismatch-dependent hMSH2-hMSH6 ATPase activity (Figure 3E, compare bar 2 with bar 5) may be progressively reduced to the background level in the absence of DNA (red line) when one and then both of the DNA ends are blocked with biotin-streptavidin (Figure 3A, compare bar 2 with bars 3 and 4 or bar 5 with bars 6 and 7). These results are consistent with previous studies that have demonstrated the hMSH2-hMSH6 ATPase is accelerated by mismatch-provoked ADP→ATP exchange and hydrolysis only occurs when hMSH2-hMSH6 translocates off a DNA end (Figure 3E, cycle A; Gradia et al., 1999). We examined the hMSH2-hMSH6 ATPase activity with the unmodified and H3(K115Ac,K122Ac)-modified single nucleosome substrates containing a biotin-streptavidin-blocked 3′ tail (Figure 3E, bars 8–11). Unlike traditional chromatin remodelers that display an increased ATPase activity with nucleosome substrates (Gangaraju and Bartholomew, 2007), we found that the ATPase activity of hMSH2-hMSH6 with the biotin-streptavidin-blocked G/T mismatch nucleosome substrates was reduced compared to G/T mismatch free DNA containing a single biotin-streptavidin-blocked end (Figure 3E; see blue bars, compare bar 3 with bars 8 and 10). As expected, the hMSH2-hMSH6 ATPase activity with the biotin-streptavidin-blocked G/T mismatch nucleosome substrates was greater than the corresponding biotin-streptavidin-blocked G/C duplex nucleosome substrates (Figure 3E, compare gray bars with blue bars or bars 8 and 10 with bars 9 and 11). Moreover, we found that the ATPase activity was greater with the H3(K115Ac,K122Ac)-modified nucleosome substrate compared to the unmodified nucleosome substrate (Figure 3E, compare bars 8 with 10). These results mirror the hMSH2-hMSH6-catalyzed chromatin remodeling studies and suggest an intimate connection between ATPase activity, a mismatch, and the ability to disassemble a nucleosome. Taken together with our previous studies (Gradia et al., 1999, 2000), we consider it likely that the ATPase activity with nucleosome substrates results from a combination of two ATPase cycles, since the product of nucleosome disassembly is a single end-blocked free-DNA substrate (Figure 3E, cycle B to cycle A via dashed blue arrow). This would explain the reduced ATPase activity, since efficient hydrolysis with nucleosome-free DNA (cycle A) would be delayed until the nucleosome was disassembled (cycle B). Alternatively, nucleosomes might enhance hMSH2-hMSH6 ATPase cycling on the DNA. However, it is hard to reconcile the catalytic enhancement of ATPase cycling by histone modifications like H3(K115Ac,K122Ac) that are buried in the nucleosome dyad.

hMSH2-hMSH6 Must Translocate along the DNA to Disassemble a Nucleosome

Chromatin remodeling proteins typically interact directly with nucleosomes (Gangaraju and Bartholomew, 2007). To determine whether hMSH2-hMSH6-catalyzed chromatin remodeling requires a mismatch to load hMSH2-hMSH6 sliding clamps that must translocate along the DNA (*cis*) or interacts directly with
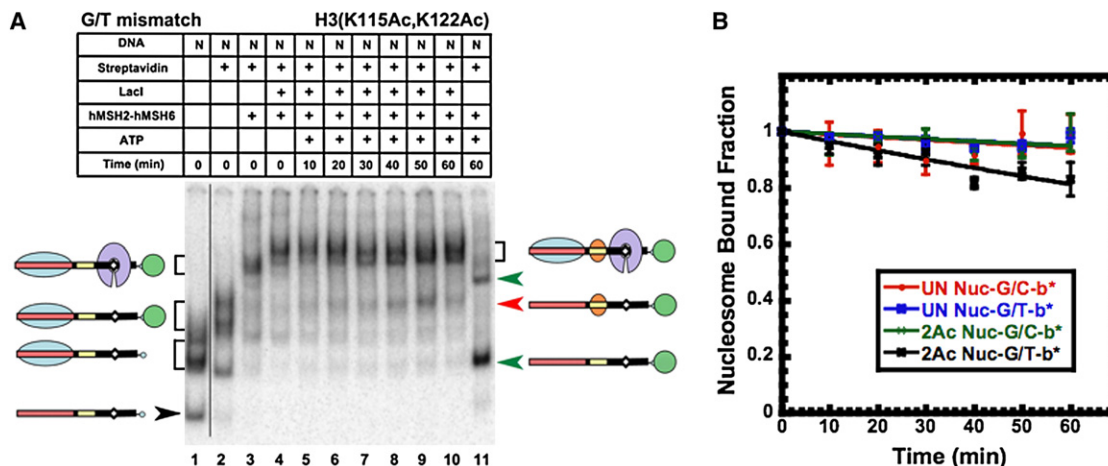
Figure 4. The Effect of Intervening LacI on hMSH2-hMSH6 Nucleosome Disassembly

(A) LacI blocks hMSH2-hMSH6 nucleosome disassembly. Black bar indicates image splicing from a single gel where spliced lanes contained redundant controls shown in Figures 2A, 2B, and 3B (lanes 6 and 7). Boxes above indicate added reaction components (+), the inclusion of free-DNA (F) or nucleosome-DNA (N), and the time of incubation (min). A schematic of DNA species with arrows or brackets indicating gel mobility position is shown on the left and right of the gel panels. The DNA substrate is colored as shown in Figure 1A with a nucleosome (blue oval), hMSH2-hMSH6 (purple clamp), streptavidin (green circle), and LacI (orange). Asterisks indicate the mobility of nucleosome-DNA substrate with bound hMSH2-hMSH6 and without a biotin-streptavidin-bound 3′ tail. Red arrow indicates the gel mobility of the nucleosome disassembly product. Green arrows are a redundant control with Figure 2B and indicate gel mobility of the nucleosome-DNA and the disassembly product following 60 min incubation without LacI.

(B) Quantitative analysis of (A) plus Figures S5A–S5C. Each data set was fit to a single exponential decay to calculate τ and $t_{1/2}$. See Figure 2 for key. Standard deviations were determined from at least three independent experiments and error bars shown (some within the symbol).

nucleosomes (*trans*), we placed a *lacO* sequence between the mismatch and the nucleosome (Figure 1A). The addition of LacI protein to a *lacO* sequence has been previously shown to provide a high-affinity block to the diffusion of MSH2-MSH6 sliding clamps (Mendillo et al., 2005). We found that the addition of LacI to the biotin-streptavidin-blocked G/T mismatch nucleosome substrate induces a near-complete inhibition of hMSH2-hMSH6-catalyzed nucleosome disassembly (Figure 4; Figure S5; $t_{1/2\ (G/T\bullet UN)}$ = 791 min, $t_{1/2\ (G/T\bullet K115Ac/K122Ac)}$ = 198 min). These results strongly suggest that the hMSH2-hMSH6 chromatin remodeling activity requires a mismatch in *cis* with the nucleosome and that hMSH2-hMSH6 must translocate from the mismatch to the nucleosome for disassembly.

DISCUSSION

Nucleosomes are disassembled in front of and reassembled behind a replication fork (Groth et al., 2007). The first fully formed nucleosome may be found approximately 250 bp behind the replication fork with intermediates in the assembly process occurring in the intervening region (Jackson, 1988; Sogo et al., 1986). Postreplication MMR is likely to be initiated in vivo shortly after a mismatch escapes the replication machinery and has been shown to form excision tracts that encompass 100–1000 bp in vitro (Fang and Modrich, 1993). These observations suggest that the human MMR machinery may encounter both fully formed nucleosomes and nucleosome assembly intermediates.

Here we have demonstrated a chromatin remodeling function for the MMR initiation heterodimer hMSH2-hMSH6. Chromatin

remodeling by hMSH2-hMSH6 requires a *cis* mismatch and translocation of the heterodimer along the DNA, ATP binding but not ATP hydrolysis, and it is enhanced by histone posttranslational modifications that increase thermal repositioning and/or reduce histone-DNA affinity. We used the 5S rDNA positioning sequence, which strongly localizes nucleosomes compared to native DNA (Thastrom et al., 1999). These observations suggest that genome-wide nucleosome disassembly by hMSH2-hMSH6 may be significantly more efficient. Moreover, artificially high-affinity nucleosome positioning sequences, such as the nonphysiological 601 positioning sequence, may mask the hMSH2-hMSH6 nucleosome disassembly process (Thastrom et al., 1999).

While we have demonstrated that the H3(K56Q) mimic of the replication-associated acetylation modification H3(K56Ac) clearly enhances nucleosome disassembly by hMSH2-hMSH6, there is growing evidence that bona fide histone acetylations additionally accelerate nucleosome thermal repositioning, which may substantially enhance hMSH2-hMSH6-dependent chromatin remodeling (Manohar et al., 2009). Moreover, SWI/SNF-independent (SIN) histone mutations that are located in the nucleosome dyad near H3(K115) and H3(K122) appear to increase the rate of nucleosome repositioning following thermal heating (Flaus et al., 2004; Muthurajan et al., 2004) and reduce DNA-histone interactions (Kurumizaka and Wolffe, 1997), thus reducing or eliminating the requirement for these chromatin remodeling factors in several DNA transactions (Kruger et al., 1995).

The rate of nucleosome disassembly ($t_{1/2}$ = 23 min) appears well within the window of MMR in vitro (Constantin et al., 2005;

Nudging

Unwrapping
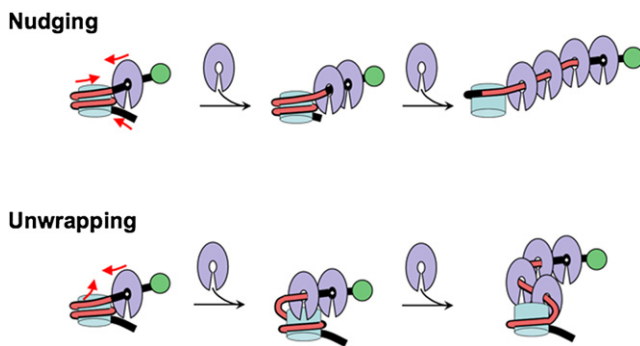
Figure 5. Two Passive Models for Chromatin Remodeling by hMSH2-hMSH6

Both models use the translocation of hMSH2-hMSH6 hydrolysis-independent sliding clamps to trap thermal fluctuations in the nucleosome structure. See text.

Zhang et al., 2005), although the rate of MMR may be somewhat reduced in the presence of nucleosomes compared to naked DNA. Our results are consistent with the conclusion that hMSH2-hMSH6 performs two important functions for MMR: (1) it specifically recognizes mismatched nucleotides to initiate repair, and (2) it creates a nucleosome-free and perhaps protein-free environment surrounding the mismatch for the excision reaction. A requirement for translocation and the lack of any detectable interaction(s) with histone components or nucleosomes strongly suggests that hMSH2-hMSH6 chromatin remodeling functions are uniquely linked to its ability to form sliding clamps. A related reaction has been considered for RAD51 polymerization-dependent chromatin remodeling (Dupaigne et al., 2008). Because chromosomes throughout phylogeny contain complex mixtures of protein-DNA, our observations might be generalized to suggest that all MSHs that form sliding clamps function similarly. Several mechanisms for MMR have been proposed and remain controversial (for review, see Kolodner et al., 2007). The Molecular Switch Model posits the mismatch-dependent loading of multiple MSH hydrolysis-independent sliding clamps that recruit MLH/PMS proteins, and connect mismatch recognition to an iterative dynamic and redundant strand excision process (Acharya et al., 2003; Gradia et al., 1997). Our observations appear to highlight an unanticipated strength of the Molecular Switch Model by suggesting that the iterative MSH hydrolysis-independent sliding clamps also perform chromatin remodeling.

Examining the role of hMSH2-hMSH6 in chromatin remodeling in vivo is complicated by the overlapping requirement for sliding clamps in both MMR and nucleosome disassembly. Thus, dissociating the hMSH2-hMSH6 chromatin remodeling activity from MMR activity has been impracticable. One prediction of our studies is that there may be a synergistic phenotype when partially defective alterations of the MMR machinery and chromatin-modifying machinery are combined. While these studies are underway, they are technically challenging and may be subtle as a result of the significant redundancies associated with histone-modification enzymes.

The absence of an energetic component associated with the translocation of hMSH2-hMSH6 sliding clamps suggests a passive mechanism for chromatin remodeling. We consider two models in which hMSH2-hMSH6 sliding clamps might *trap* inherent structural fluctuations in nucleosomes leading to disassembly (Figure 5). One model proposes that the formation of iterative sliding clamps may capture thermally induced position shifts of the nucleosome away from the mismatch, ultimately "nudging" the nucleosome off the open end of our model DNA substrates (Figure 5). Since free DNA ends are rare in vivo, such a Nudging Model would be envisioned to detain nucleosomes away from the mismatch along the DNA. A second model considers thermal fluctuations (breathing) by the nucleosome-DNA (Li and Widom, 2004; Polach and Widom, 1995), which might be irreversibly captured in the open state by hMSH2-hMSH6 sliding clamps (Figure 5). In this Unwrapping Model, hMSH2-hMSH6 sliding clamps would iteratively occupy the DNA of a breathing nucleosome, beginning at the entry-exit region, until a critical DNA length is engaged and the nucleosome spontaneously disassembles. Both models do not appear to be mutually exclusive and may occur in concert. Passive chromatin remodeling has been considered for transcription factors where binding sites are occluded by nucleosomes (Polach and Widom, 1995). However, nucleosome disassembly by hMSH2-hMSH6 appears considerably different since it requires the formation of autonomous energy-independent translocating protein clamps on the DNA. Regardless of the detailed mechanics, it appears that hMSH2-hMSH6 typifies a class of passive DNA lesion-dependent chromatin remodeling factors.

EXPERIMENTAL PROCEDURES

Protein and DNA Substrates

hMSH2-hMSH6 and the hMSH2(K675A)-hMSH6(K1140A) were purified as previously described (Gradia et al., 1997). LacI protein was a generous gift from Dr. Kathleen Matthews (Rice University). The G/C and G/T oligonucleotides (5′-GCTTAGGATCATCGAGGATC**G**AGCTCGGTGCAATTCAGCGGG-3′ with the complementary strand 5′-TCGACCCGCTGAATTGCACCGAGCT(**T/C**)GATCCTCGATGATCCTAAGC-3′ containing a 3′ biotin moiety) were synthesized (Midland Certified Research Company), annealed, and purified by HPLC using a Waters Gen-Pak column (Gradia et al., 1997). The site of the mismatch is indicated in bold. The *Xenopus* 5S rDNA nucleosome localization sequence containing the *lacO* sequence (5′-TGGAATTGTGAGCGGATAAC AATT-3′) on the 3′ end was amplified by PCR from a pBluescript (SK−) plasmid containing the *Xenopus* 5S rDNA sequence using tailed primers (5′-G**CCCG GG**GGATCCACTAGTTC-3′; 5′-ACCGCCTGGGCCTGGTAC*AATTGTTATCCG CTCACAATTCCA***CTCGAG**CGA-3′). The PCR product (5S rDNA plus the *lacO* sequence) was digested with XhoI on the 3′ end and SmaI on the 5′ end. The annealed synthetic oligonucleotide containing a G/C duplex or G/T mismatch was ligated to the PCR product, purified by native PAGE, and verified by restriction analysis.

Preparation of Site-Specific Acetylated Histone H3

Histone H3 acetylated at K115 and K122 was prepared by expressed protein ligation (Manohar et al., 2009). A peptide containing amino acids 110–135 was synthesized manually on Boc-Ala-PAM resin (Novabiochem) using standard Boc-N$^{\alpha}$ protection strategies and HBTU activation protocols. K115 and K122 were acetylated prior to HF cleavage from the resin and purified by RP-HPLC. Truncated histone H3 (residues 1–109) was cloned as a fusion protein with the GyrA intein into the pTXB1 vector (New England Biolabs). The H3-intein fusion protein was expressed in *E. coli* BL21 (DE3) cells and purified from inclusion bodies by ion exchange and gel filtration chromatography. The purified protein was refolded by dialysis into a high-salt buffer. Thiolysis was then initiated by addition of 100 mM MESNA (mercaptoethanesulfonic

acid) and allowed to continue for 24 hr at 4°C. The buffer components were then adjusted to generate protein-ligation buffer I (50 mM HEPES [pH 7.5], 6 M urea, 1 M NaCl, 1 mM EDTA, 50 mM MESNA) and the protein concentrated to >1 mg/mL of the thioester and stored at –80°C. Expressed protein ligation was done with ten molar equivalents of the acetylated H3(110–135) peptide to the H3(1–109) thioester in protein ligation buffer II (50 mM HEPES [pH 7.5], 6 M urea, 1 M NaCl, 1 mM EDTA, 20 mM TCEP), which proceeded overnight at room temperature with gentle agitation. Full-length semisynthetic H3 was then purified by ion exchange chromatography over a TSKgel SP-5PW column (TOSOH Bioscience).

Histone Octamer Preparation

Recombinant unmodified histones H2A, H2B, H3, and H4 were expressed and purified as previously described (Luger et al., 1999). The unmodified, H3(K56Q), and H3(K115Ac,K122Ac) histones were unfolded separately in 7 M guanidine, 20 mM Tris (pH 7.5), and 10 mM DTT for 1–3 hr and then spun to remove aggregates. The four core histones were combined at equal molar ratio with total histone concentration adjusted to 5 mg/ml in 200 ul. The octamer was refolded by double dialysis in 2 M NaCl, 10 mM Tris-HCl (pH 7.5), 1 mM EDTA, and 5 mM BME. The recovered refolded octamer was centrifuged to remove large aggregates and then purified over a Superdex 200 (GE healthcare) column. The purity of each octamer was confirmed by SDS-PAGE and mass spectrometry.

Nucleosome Reconstitution

Nucleosomes were reconstituted with ^{32}P-labeled nucleosome-DNA substrate (Figure 1A) and with octamer containing unmodified, H3(K56Q), or H3(K115Ac,K122Ac) histones by salt double dialysis as previously described (Thastrom et al., 2004). The reconstituted nucleosomes were purified by ultracentrifugation on a 5%–30% sucrose gradient. Fractions corresponding to the peak of reconstituted nucleosomes were pooled and concentrated in a Centricon 30 concentrator (Amicon) and washed twice with 0.5 × TE. The nucleosome purity was verified with a 5% native polyacrylamide gel containing 1/3 × TBE.

Binding Studies and ATPase

Reactions were performed in 25 mM HEPES (pH 7.8), 15% glycerol, 100 mM NaCl, 1 mM DTT, and 2 mM MgCl$_2$ containing 20 ng/µL poly dI-dC, 200 µg/mL acetylated BSA (Promega), and approximately 5 fmol of ^{32}P-labeled mononucleosome or the 265 bp free-DNA substrate in a final volume of 20 µl. hMSH2-hMSH6 (at the indicated concentration) was preincubated with the nucleosome-DNA on ice for 10 min. Reactions were separated on a 5% native polyacrylamide/5% glycerol in 1/3 × TBE at 4°C for 3 hr. Gels were dried, quantified by phosphorimager (Molecular Dynamics), and represented as percent substrate shifted. Standard deviation was calculated from at least three separate experiments. The ATPase activity was determined in 25 mM HEPES (pH 7.8), 100 mM NaCl, 10 mM MgCl$_2$, 1 mM DTT, 0.01 mM EDTA, 15% glycerol, 200 µg/mL acetylated BSA (Promega), 500 µM unlabeled ATP, and 16.5 nM [γ-^{32}P]-ATP in a final volume of 20 µl. Steady-state reactions were performed using 25 nM hMSH2-hMSH6 and 25 nM free-DNA, nucleosome-DNA or without DNA as indicated. We determined that ATP hydrolysis was linear under these conditions for at least 2 hr. Reactions were incubated at 37°C for 60 min and processed as described previously (Gradia et al., 1997).

Chromatin Remodeling

Reactions were performed in 25 mM HEPES (pH 7.8), 15% glycerol, 100 mM NaCl, 1 mM DTT, 5 mM MgCl$_2$, 20 ng/µL poly dI-dC, 200 µg/mL acetylated BSA, and approximately 5 fmol of ^{32}P-labeled nucleosome-DNA in a 20 µl reaction volume. Where indicated, 900 nM of streptavidin was included for 5 min on ice prior to the addition of hMSH2-hMSH6 or hMSH2(K675A)-hMSH6(K1140A). Reactions were incubated with hMSH2-hMSH6 (250 nM) or hMSH2(K675A)-hMSH6(K1140A) (250 nM) on ice for 10 min. Where indicated, 4 nM LacI was incubated with the nucleosome-DNA for 10 min on ice prior to the addition of hMSH2-hMSH6. Dissociation with 1 mM ATP (or ATPγS) was performed where indicated by addition of nucleotide and a further incubation from 10 to 60 min at 37°C. The reactions were separated on a 5% native polyacrylamide/5% glycerol gel in 1/3 × TBE at 4°C for 3 hr. Gels were dried and quantified by phosphorimager (Molecular Dynamics). Standard deviations were calculated from at least three independent experiments.

REFERENCES

Acharya, S., Foster, P.L., Brooks, P., and Fishel, R. (2003). The coordinated functions of the *E. coli* MutS and MutL proteins in mismatch repair. Mol. Cell *12*, 233–246.

Ataian, Y., and Krebs, J.E. (2006). Five repair pathways in one context: chromatin modification during DNA repair. Biochem. Cell Biol. *84*, 490–504.

Boland, C.R., and Fishel, R. (2005). Lynch syndrome: form, function, proteins, and basketball. Gastroenterology *129*, 751–755.

Constantin, N., Dzantiev, L., Kadyrov, F.A., and Modrich, P. (2005). Human mismatch repair: reconstitution of a nick-directed bidirectional reaction. J. Biol. Chem. *280*, 39752–39761.

Drummond, J.T., Li, G.M., Longley, M.J., and Modrich, P. (1995). Isolation of an hMSH2-p160 heterodimer that restores DNA mismatch repair to tumor cells. Science *268*, 1909–1912.

Dupaigne, P., Lavelle, C., Justome, A., Lafosse, S., Mirambeau, G., Lipinski, M., Pietrement, O., and Le Cam, E. (2008). Rad51 polymerization reveals a new chromatin remodeling mechanism. PLoS ONE *3*, e3643. 10.1371/journal.pone.0003643.

English, C.M., Adkins, M.W., Carson, J.J., Churchill, M.E., and Tyler, J.K. (2006). Structural basis for the histone chaperone activity of Asf1. Cell *127*, 495–508.

Escargueil, A.E., Soares, D.G., Salvador, M., Larsen, A.K., and Henriques, J.A. (2008). What histone code for DNA repair? Mutat. Res. *658*, 259–270.

Fang, W.H., and Modrich, P. (1993). Human strand-specific mismatch repair occurs by a bidirectional mechanism similar to that of the bacterial reaction. J. Biol. Chem. *268*, 11838–11844.

Flaus, A., Rencurel, C., Ferreira, H., Wiechens, N., and Owen-Hughes, T. (2004). Sin mutations alter inherent nucleosome mobility. EMBO J. *23*, 343–353.

Friedberg, E.C., Walker, G.C., Siede, W., Wood, R.D., Schultz, R.A., and Ellenberger, T. (2006). DNA Repair and Mutagenesis, Second Edition (Washington, D.C.: American Society of Microbiology).

Gangaraju, V.K., and Bartholomew, B. (2007). Mechanisms of ATP dependent chromatin remodeling. Mutat. Res. *618*, 3–17.

Gradia, S., Acharya, S., and Fishel, R. (1997). The human mismatch recognition complex hMSH2-hMSH6 functions as a novel molecular switch. Cell *91*, 995–1005.

Gradia, S., Subramanian, D., Wilson, T., Acharya, S., Makhov, A., Griffith, J., and Fishel, R. (1999). hMSH2-hMSH6 forms a hydrolysis-independent sliding clamp on mismatched DNA. Mol. Cell *3*, 255–261.

Gradia, S., Acharya, S., and Fishel, R. (2000). The role of mismatched nucleotides in activating the hMSH2-hMSH6 molecular switch. J. Biol. Chem. *275*, 3922–3930.

Groth, A., Rocha, W., Verreault, A., and Almouzni, G. (2007). Chromatin challenges during DNA replication and repair. Cell *128*, 721–733.

Haber, L.T., and Walker, G.C. (1991). Altering the conserved nucleotide binding motif in the Salmonella typhimurium MutS mismatch repair protein affects both its ATPase and mismatch binding activities. EMBO J. *10*, 2707–2715.

Hyland, E.M., Cosgrove, M.S., Molina, H., Wang, D., Pandey, A., Cottee, R.J., and Boeke, J.D. (2005). Insights into the role of histone H3 and histone H4 core modifiable residues in Saccharomyces cerevisiae. Mol. Cell. Biol. *25*, 10060–10070.

Jackson, V. (1988). Deposition of newly synthesized histones: hybrid nucleosomes are not tandemly arranged on daughter DNA strands. Biochemistry *27*, 2109–2120.

Kolodner, R.D., Mendillo, M.L., and Putnam, C.D. (2007). Coupling distant sites in DNA during DNA mismatch repair. Proc. Natl. Acad. Sci. USA *104*, 12953–12954.

Kruger, W., Peterson, C.L., Sil, A., Coburn, C., Arents, G., Moudrianakis, E.N., and Herskowitz, I. (1995). Amino acid substitutions in the structured domains of histones H3 and H4 partially relieve the requirement of the yeast SWI/SNF complex for transcription. Genes Dev. *9*, 2770–2779.

Kurumizaka, H., and Wolffe, A.P. (1997). Sin mutations of histone H3: influence on nucleosome core structure and function. Mol. Cell. Biol. *17*, 6953–6969.

Li, G., and Widom, J. (2004). Nucleosomes facilitate their own invasion. Nat. Struct. Mol. Biol. *11*, 763–769.

Lowary, P.T., and Widom, J. (1998). New DNA sequence rules for high affinity binding to histone octamer and sequence-directed nucleosome positioning. J. Mol. Biol. *276*, 19–42.

Luger, K., Rechsteiner, T.J., and Richmond, T.J. (1999). Preparation of nucleosome core particle from recombinant histones. Methods Enzymol. *304*, 3–19.

Manohar, M., Mooney, A.M., North, J., Nakkula, R.J., Picking, J.W., Edon, A., Fishel, R., Poirier, M.G., and Ottesen, J.J. (2009). DNA-histone binding affinity is reduced by acetylation of histone H3 at the nucleosome dyad. J. Biol. Chem. *284*, 23312–23321.

Mazurek, A., Johnson, C.N., Germann, M.W., and Fishel, R. (2009). Sequence context effect for hMSH2-hMSH6 mismatch-dependent activation. Proc. Natl. Acad. Sci. USA *106*, 4177–4182.

Mendillo, M.L., Mazur, D.J., and Kolodner, R.D. (2005). Analysis of the interaction between the Saccharomyces cerevisiae MSH2-MSH6 and MLH1-PMS1 complexes with DNA using a reversible DNA end-blocking system. J. Biol. Chem. *280*, 22245–22257.

Muthurajan, U.M., Bao, Y., Forsberg, L.J., Edayathumangalam, R.S., Dyer, P.N., White, C.L., and Luger, K. (2004). Crystal structures of histone Sin mutant nucleosomes reveal altered protein-DNA interactions. EMBO J. *23*, 260–271.

Polach, K.J., and Widom, J. (1995). Mechanism of protein access to specific DNA sequences in chromatin: a dynamic equilibrium model for gene regulation. J. Mol. Biol. *254*, 130–149.

Schofield, M.J., Nayak, S., Scott, T.H., Du, C., and Hsieh, P. (2001). Interaction of Escherichia coli MutS and MutL at a DNA mismatch. J. Biol. Chem. *276*, 28291–28299.

Selmane, T., Schofield, M.J., Nayak, S., Du, C., and Hsieh, P. (2003). Formation of a DNA mismatch repair complex mediated by ATP. J. Mol. Biol. *334*, 949–965.

Sogo, J.M., Stahl, H., Koller, T., and Knippers, R. (1986). Structure of replicating simian virus 40 minichromosomes. The replication fork, core histone segregation and terminal structures. J. Mol. Biol. *189*, 189–204.

Thastrom, A., Lowary, P.T., Widlund, H.R., Cao, H., Kubista, M., and Widom, J. (1999). Sequence motifs and free energies of selected natural and non-natural nucleosome positioning DNA sequences. J. Mol. Biol. *288*, 213–229.

Thastrom, A., Lowary, P.T., and Widom, J. (2004). Measurement of histone-DNA interaction free energy in nucleosomes. Methods *33*, 33–44.

Utley, R.T., Owen-Hughes, T.A., Juan, L.J., Cote, J., Adams, C.C., and Workman, J.L. (1996). In vitro analysis of transcription factor binding to nucleosomes and nucleosome disruption/displacement. Methods Enzymol. *274*, 276–291.

Yoshioka, K., Yoshioka, Y., and Hsieh, P. (2006). ATR kinase activation mediated by MutSalpha and MutLalpha in response to cytotoxic O6-methylguanine adducts. Mol. Cell *22*, 501–510.

Zhang, L., Eugeni, E.E., Parthun, M.R., and Freitas, M.A. (2003). Identification of novel histone post-translational modifications by peptide mass fingerprinting. Chromosoma *112*, 77–86.

Zhang, Y., Yuan, F., Presnell, S.R., Tian, K., Gao, Y., Tomkinson, A.E., Gu, L., and Li, G.M. (2005). Reconstitution of 5′-directed human mismatch repair in a purified system. Cell *122*, 693–705.